

How does sea ice influence $\delta^{18}O$ of Arctic precipitation?

Anne-Katrine Faber¹, Bo Møllersøe Vinther¹, Jesper Sjolte², and Rasmus Anker Pedersen^{1,3}

¹Centre for Ice and Climate, Niels Bohr Institute, University of Copenhagen, Copenhagen, Denmark

²Department of Geology, Quaternary Sciences, Lund University, Lund, Sweden

³Climate and Arctic Research, Danish Meteorological Institute, Copenhagen, Denmark

Correspondence to: Anne-Katrine Faber (akfaber@nbi.ku.dk)

Abstract. This study investigates how variations in Arctic sea ice and sea surface conditions influence $\delta^{18}O$ of present-day Arctic precipitation. This is done using the model isoCAM3, an isotope-equipped version of the National Center for Atmospheric Research Community Atmosphere Model version 3. Four sensitivity experiments and one control simulation are performed with prescribed SST and sea ice. Each of the four experiments simulates the atmospheric and isotopic response to Arctic oceanic conditions for selected years after the beginning of the satellite era in 1979.

Changes in sea ice extent and sea surface temperatures have different impact in Greenland and the rest of the Arctic. The simulated changes in central Arctic sea ice do not influence $\delta^{18}O$ of Greenland precipitation, only anomalies of Baffin Bay sea ice. However, this does not exclude that simulations based on other sea ice and sea surface temperature distributions might yield changes in Greenland $\delta^{18}O$ of precipitation. For the Arctic, $\delta^{18}O$ of precipitation and water vapour is sensitive to local changes of sea ice and sea surface temperature and the changes in water vapour are surface based. Reduced sea ice extent yields more enriched isotope values, while increased sea ice extent yields more depleted isotope values. The distribution of the sea ice and sea surface conditions is found to be essential for the spatial distribution of the simulated changes in $\delta^{18}O$.

1 Introduction

Records of stable water isotopologues from polar ice cores have been widely used to reconstruct past climate variability. Since the pioneering work by Dansgaard (1964), the understanding of stable water isotopologues as a proxy for temperature has significantly advanced. It has become clear that the isotopic composition of precipitation is a complex signal, influenced by both local and regional climate conditions (Vinther et al., 2010; Steen-Larsen et al., 2011; Sjolte et al., 2011; Sodemann et al., 2008b; White et al., 1997; Johnsen et al., 1989). The isotopic composition of the precipitation is an integrated signal of the conditions along the moisture transport pathway from source to deposition.

As a result, there is a need for a detailed process-based understanding of the factors that can alter the isotopic composition of the transported moisture.

Studies using models, ice cores, snow and water vapour measurements have investigated the physical and dynamical processes influencing the isotopic composition of precipitation. Variations in local Greenland temperatures, conditions at source regions and atmospheric circulation all influence the isotopic composition of Greenland precipitation (Steen-Larsen et al., 2011; Bonne et al., 2014; Sodemann et al., 2008a, b; Sjolte et al., 2011; Vinther et al., 2010).

Several model studies highlight sea ice changes as important for understanding changes in the isotopic composition of precipitation. Sea ice changes in the Arctic were investigated during Dansgaard-Oeschger events (Li et al., 2010) and for exceptionally warm climates (Sime et al., 2013). For Antarctica, the impact of sea ice changes were studied using idealized reductions of the circular shaped sea ice cover (Noone, 2004). None of these model studies investigate sea ice perturbations comparable to present-day observations. Measurements from ice cores spanning this period suggest that sea ice changes can influence the isotopic composition of precipitation (Divine et al., 2011; Opel et al., 2013; Ku et al., 2012; Fauria et al., 2010).

A study of idealised changes of Antarctic sea ice show a non-uniform spatial distribution of the modelled isotopic response over Antarctica (Noone, 2004). The heterogeneity of the response is suggested to reflect the existence of different processes driving local and long range moisture transport to coastal and high elevation regions of Antarctica. Due to differences in the configuration of landmasses, open ocean and sea ice, it is difficult to directly transfer findings of Noone (2004) from Antarctic to the Arctic.

The impact of changes in sea ice and connected sea surface temperatures (SST) of the Arctic ocean were studied by Sime et al. (2013). The sea ice conditions were created using an experiment where a coupled climate model was forced by respectively $2\times$, $4\times$ and $8\times$ CO_2 . Hereafter the sea ice and SST conditions were used to force the applied atmospheric isotope models. Differences in the configurations of sea ice extent and SST were found to be essential for the resulting large variability in the isotope-temperature slope of $0.1 - 0.7 \text{‰}/\text{C}$ for the Greenland ice sheet. While these CO_2 changes used by Sime et al. (2013) do not allow direct comparison with present-day Arctic conditions, the results highlight processes that might be important for present day climate.

The recent decades of rapid Arctic sea ice decline provides an interesting opportunity to study how $\delta^{18}\text{O}$ responds to realistic changes of sea ice and sea surface temperatures of present-day climate. We here present results from isoCAM3 model simulations forced with observed Arctic sea ice and sea surface temperature (SST) conditions derived from observations. This paper will address how the sea ice and sea surface conditions influence the $\delta^{18}\text{O}$ in precipitation in the Arctic, and the role of the spatial configuration of the sea surface changes. The structure of the paper is as follows; (1) The model and experiments are described, (2) Results of the simulations are presented, (3) The influence of atmospheric moisture processes is discussed.

2 Experimental configuration

2.1 The model isoCAM3

The simulations of the isotopic composition of precipitation and water vapour in this study are conducted with isoCAM3. This is an atmospheric general circulation model (AGCM) enabled with the ability to trace the various species of water isotopologues. The model is based on the Community Atmosphere Model version 3 (CAM3) (Collins et al., 2006), and the isotope module was developed by David Noone, University of Colorado. More details of isoCAM3 can be found in Noone and Sturm (2010) The model isoCAM3 has been applied in several studies that investigated the isotopic response to past climate changes (Tharammal et al., 2013; Speelman et al., 2010; Sturm et al., 2010; Pausata et al., 2011; Liu et al., 2012; Sewall and Fricke, 2013; Liu et al., 2014).

The horizontal resolution of the model is T85 ($\sim 1.4^\circ \times 1.4^\circ$) with 26 hybrid-sigma levels in the vertical. In this study the SST and sea ice concentrations are specified, thus the only surface temperatures that are calculated interactively are land and sea ice surface temperatures. This configuration allows no feedback between atmospheric circulation and open ocean SST. Greenhouse gases, vegetation, ice sheets are all set to modern conditions. More specifically greenhouse gasses are set to the following CAM3 default levels (year 1990): CO₂: 355 (ppmv), CH₄: 1714 (ppbv), N₂O: 311 (ppbv). The solar constant is set to 1365 (Wm^{-2}) and orbital configurations are set to the year 1850.

2.2 Ensemble design

We perform a set of four sensitivity experiments and one control simulation to investigate how observed variations in Arctic sea surface conditions influences $\delta^{18}O$. Every model integration is run for 15 years (following one year for spin-up). Each of the four sensitivity experiments simulates the $\delta^{18}O$ response to sea ice concentration and sea surface temperature (SST) for selected years in the time period 1979-2013 within the satellite era. The 12-month time periods are selected based on the four most extreme cases of high and low September sea ice extent recorded during the time period (1979-2012) by the NSIDC Sea ice Index (Fetterer et al., 2002, updated daily). The control simulation (CTRL) simulates the $\delta^{18}O$ response using the 12 months climatology of sea ice concentration and SST for the full time period April 1979 to March 2013. Only the Arctic oceanic surface boundary conditions differ between the runs. An overview of the model experiments are given in Tab. 1.

We force the model isoCAM3 with an annual cycle of monthly mean SST and sea ice conditions obtained from ERA-Interim (Dee et al., 2011). This annual cycle goes from April to March thus spanning the full sea ice cycle related to the selected cases of September sea ice extent. Hereafter the model runs for 15 years (following one year of spin up) with repeated annual cycle. All re-analysis data are interpolated bilinearly from the ERA-Interim ($1^\circ \times 1^\circ$) to the CAM3 T85 resolution, and hereafter checked for consistency.

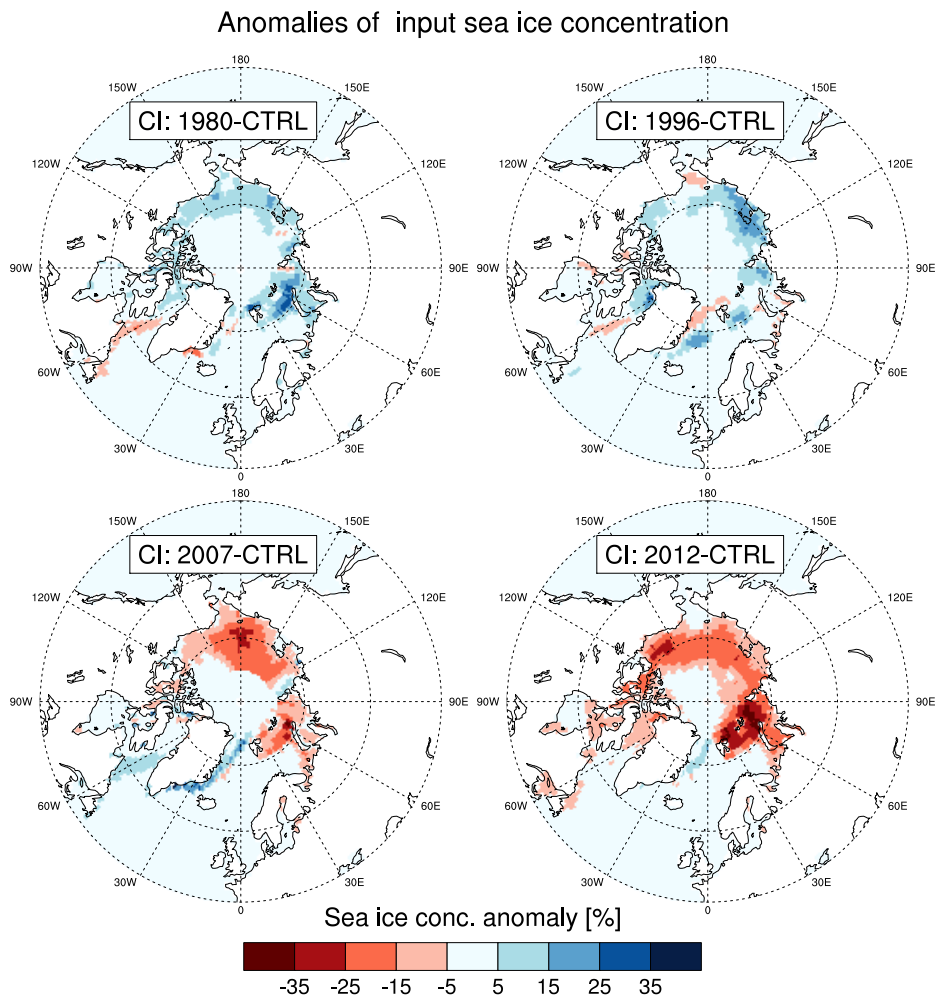


Figure 1. Annual mean anomalies of sea ice concentration (CI) used to force the model

See tab. 1 for details. Red colours represent a decrease in sea ice compared to the CTRL run. Blue colours represent an increase in sea ice compared to the CTRL run (mean April 1979 to March 2013).

Anomalies of input of SST

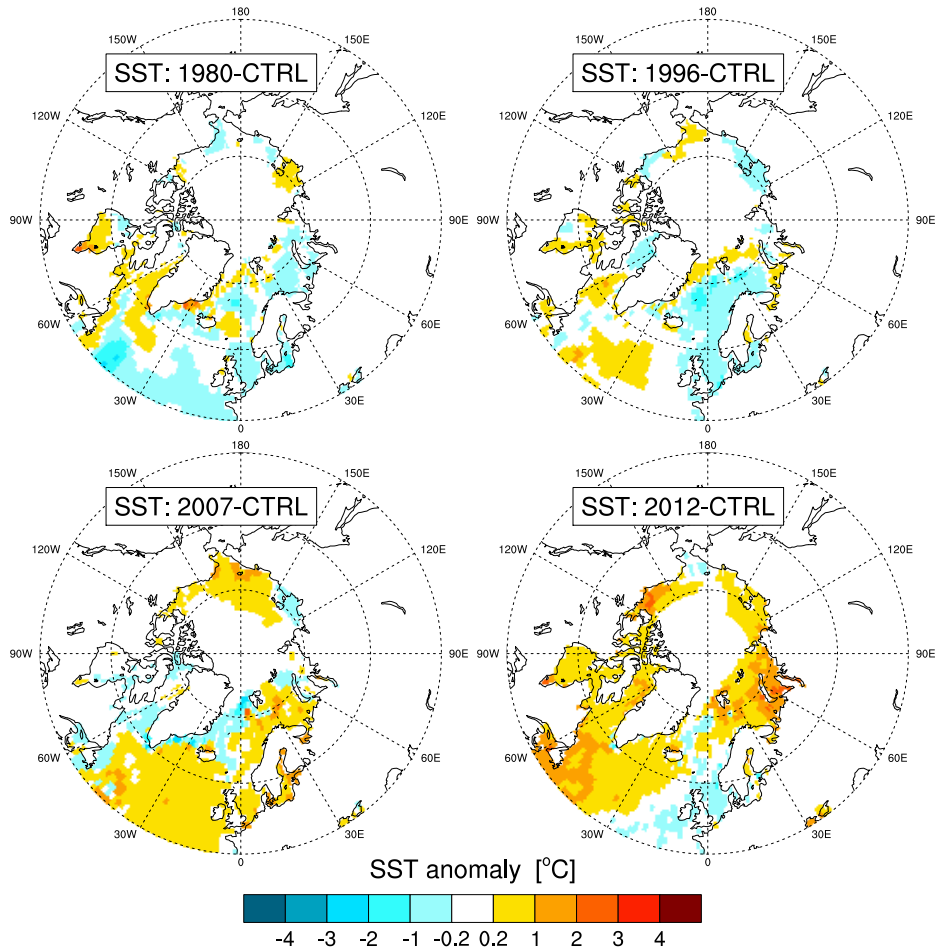


Figure 2. Annual mean anomalies of sea surface temperature (SST) used to force the model

See tab. 1 for details. Red and yellow colours represent a increase in SST compared to the CTRL run. Blue colours represent a decrease in SST compared to the CTRL run (mean April 1979 to March 2013).

Overview of model experiments

Experiment	Prescribed SST and sea ice
"1980"	ERA-Interim monthly mean: April 1980-March 1981
"1996"	ERA-Interim monthly mean: April 1996-March 1997
"2007"	ERA-Interim monthly mean: April 2007-March 2008
"2012"	ERA-Interim monthly mean: April 2012-March 2013
CTRL	ERA-Interim monthly mean climatology: April 1979-March 2013

Table 1. Overview of model experiments

Changes in Arctic SST are in nature an inseparable part of the sea ice changes. Keeping the SST constant and only simulating the atmospheric response to sea ice changes, would therefore lead to unrealistic temperature gradients (see Screen et al. (2013b) for further discussion on this topic). Therefore, we chose that these experiments are based on both changes in sea ice and SST. A masking of the SST data is applied to eliminate remote influences from extra-polar climate patterns (e.g. from the El Niño Southern Oscillation or Pacific Decadal Oscillation). This masking is constructed so that only the conditions near the Arctic differ from experiment to experiment. Hence, this global ocean data is divided in an Arctic and a non-Arctic region. The Arctic region refers to the region of ocean/sea ice conditions expected to influence the Arctic climate and is therefore rather semi-Arctic. Due the geographical configuration of the continents it is chosen to confine this region with southern boundaries of $66^{\circ}N$ and $37^{\circ}N$ for the Pacific and Atlantic sector respectively. The relatively southern definition of the semi-Arctic region in the North Atlantic is chosen to also include the southern-most position of sea ice export in the Newfoundland area.

Each experiment is forced by different SST and sea ice conditions in the (semi-)Arctic region corresponding to the values for the selected year. The non-Arctic part of the dataset is identical for all the different experiments and has values from the mean climatology of ERA-Interim 1979-2012. The area between the Arctic and non-Arctic part in the North Atlantic has strong naturally occurring SST gradients. To avoid smoothing of natural SST gradients, no smoothing is applied to the constructed oceanic data set. The sea ice concentrations and SST used to force the model are shown in Fig. 1 and Fig. 2 here displayed as annual mean anomalies between the respective experiment and the CTRL run.

3 Atmospheric response to changes in sea ice extent

3.1 Atmospheric response

Changes in sea ice concentration and SST force a strong local response in surface air temperature
120 (T_{2m}) (see Fig. 3) with cooling where sea ice extent is increased, and warming where sea ice extent
is decreased. The simulated temperature changes are in agreement with other modelling studies that
have investigated the atmospheric response to prescribed reanalysis-based changes (Screen et al.
(2013a); Magnusdottir et al. (2004); Blüthgen et al. (2012), see also reviews Budikova (2009); Bader
et al. (2011)). Changes in annual mean precipitation amount are found negligible (see appendix).

125 3.2 Isotopic response

The CTRL run is compared to values of $\delta^{18}O$ observations from ice cores and GNIP stations for
Greenland and a positive bias is found (see figure in appendix). As a consequence this study only in-
vestigates anomalies and not absolute values. All sensitivity experiments clearly show that changes
in sea surface conditions influence the modelled $\delta^{18}O$ of Arctic precipitation (Fig. 4). Decreased
130 (increased) sea ice concentration and connected SST results in enriched (depleted) $\delta^{18}O$ values of
precipitation (hereafter referred to as $\delta^{18}O_p$). Annual means of $\delta^{18}O_p$ are computed as precipita-
tion weighted annual means. The spatial distribution of changes in $\delta^{18}O_p$ is similar to the spatial
distribution of changes in simulated surface air temperature.

This shows that the spatial response of the simulated $\delta^{18}O_p$ to changes in sea surface conditions is
135 controlled by the distribution of these changes. The distribution of the $\delta^{18}O_p$ response to the ocean
conditions depends on the sea ice and SST configuration in the different experiments. As shown
in Fig. 4 the $\delta^{18}O_p$ of the precipitation over central part of Greenland appears unaffected by the
simulated changes in sea ice cover in all experiments whereas $\delta^{18}O_p$ changes over the Pacific-Arctic
and the Barents/Kara Sea region depend on the distribution of sea ice in the given experiment.

140 The experiments "1980" and "1996" both have increased sea ice extent and colder SSTs compared
to the CTRL experiments, yet the spatial distributions of the sea surface conditions in the Arctic
Ocean are very different. This is observed in the Barents/Kara Sea region, in the Baffin Bay and near
the northern coast of Greenland. The corresponding isotopic response match the differences in the
spatial pattern observed in the sea ice cover.

145 The two experiments with low sea ice extent compared to the CTRL experiments (the "2007"
and "2012" experiments) similarly show that the sea ice distribution is important for $\delta^{18}O_p$. The
Labrador/Baffin region does not experience any significant change in the isotopic composition of
precipitation in the "2007" experiment. Conversely, significant changes are simulated in the "2012"
experiment where the sea ice changes in this region are much more pronounced. For the Barents Sea
150 region both experiments yield positive $\delta^{18}O_p$ anomalies, but the amplitude of the anomalies are dif-
ferent. Interestingly, this difference in amplitudes is also found in the sea ice concentration anomalies

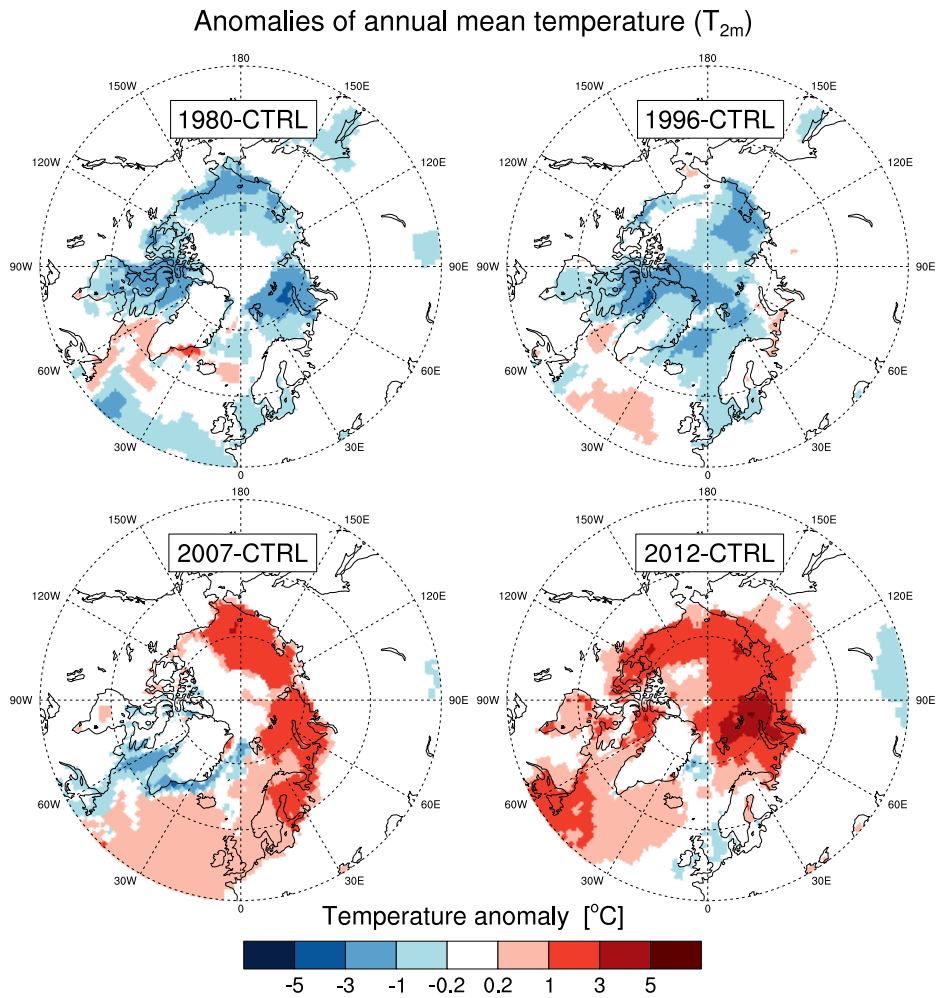


Figure 3. Annual mean anomalies of surface air temperatures (T_{2m})

Annual mean anomalies for the four simulations compared to the CTRL run. Red colours represent a increase in T_{2m} compared to the CTRL run. Blue colours represent a decrease in T_{2m} compared to the CTRL run. Only anomalies statistically significant at the 95% confidence level are shown.

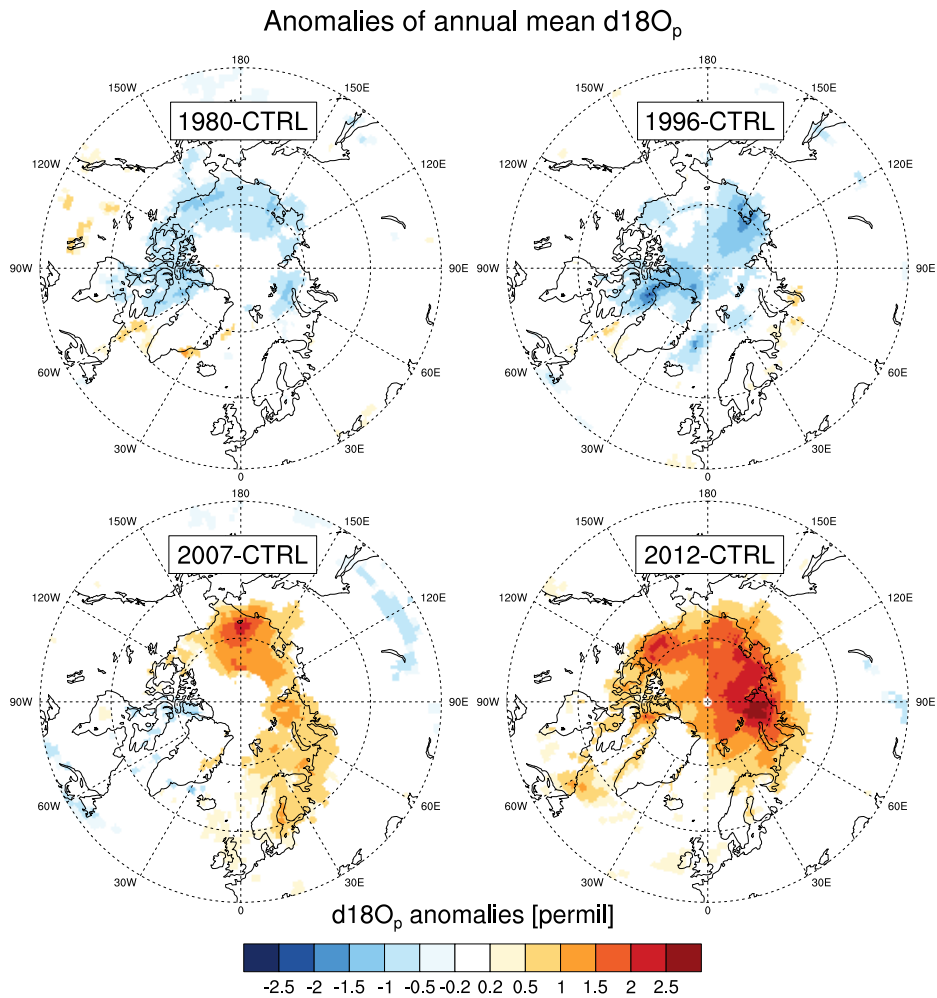


Figure 4. Annual mean anomalies of $\delta^{18}O$ of precipitation ($\delta^{18}O_p$)

Annual mean anomalies for the four simulations compared to the CTRL run. Only anomalies statistically significant at the 95% confidence level are shown. Red and yellow colours represent an increase in $\delta^{18}O_p$ compared to the CTRL run. Blue colours represent a decrease in $\delta^{18}O_p$ compared to the CTRL run.

used to simulate the isotopic response. Thus this suggests that both distribution and magnitude of the changes in sea surface conditions are important for the change in $\delta^{18}O_p$.

3.3 $\delta^{18}O_p$ -temperature relationship

155 From a climate reconstruction perspective it is interesting to examine whether the isotope-temperature relationship ($\delta^{18}O_p$ -T) is sensitive to changes in sea ice cover and SST. Scatter plots of annual mean anomalies of $\Delta\delta^{18}O_p$ - ΔT are shown in Fig. 5. Only grid points in the Arctic ($60^\circ N$ - $90^\circ N$) are included in the analysis.

160 Linear regression shows that the spatial $\Delta\delta^{18}O_p$ - ΔT slopes for each of the experiment all are within the range of 0.38 to 0.53 $\text{‰}/^\circ C$. Linear regression for all experiments together (Fig. 5 "All experiments") show a larger range of values of anomalies and yields a slope of 0.57 $\text{‰}/^\circ C$ with $R^2 = 0.761$. For experiments with high sea ice extent the slope is 0.38 $\text{‰}/^\circ C$ with $R^2 = 0.59$ for "1980" and 0.53 $\text{‰}/^\circ C$ with $R^2 = 0.575$ for "1996". For experiments with low sea ice extent the value of the slope is 0.42 $\text{‰}/^\circ C$ with $R^2 = 0.732$ for "2007" and 0.48 $\text{‰}/^\circ C$ with $R^2 = 0.635$ for 165 "2012".

In this study, the slope of $\delta^{18}O_p$ -T relationship is found to be insensitive to changes in the perturbations of sea ice. Differences in the intercept values of the regression are noted, most pronounced for the experiment "2012" where the offset of $\Delta\delta^{18}O_p$ is -0.39‰ .

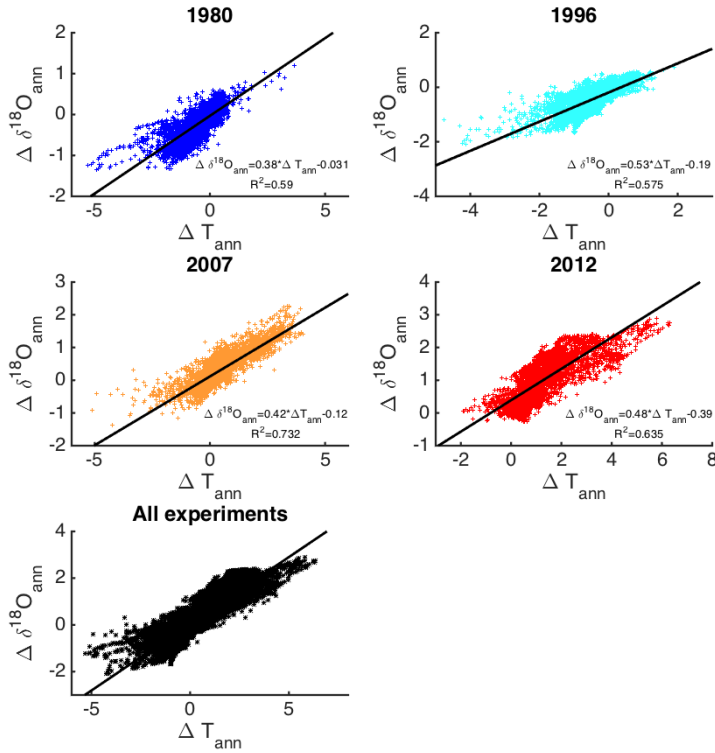


Figure 5. Scatter plots of anomalies of annual mean surface temperature (ΔT) versus $\Delta \delta^{18}O_p$ anomalies

The plots show scatterplots of all grid points from $60^\circ N - 90^\circ N$ for the different experiments compared to CTRL. The colours refer to the different experiments. Dark blue refers to experiment "1980", light blue to experiment "1996", orange to experiment "2007" and red to experiment "2012". Black colors show results from all experiments. Note that the scale of the x and y-axes are different for each plot.

3.4 Atmospheric moisture processes

170 The $\delta^{18}O_p$ response to sea ice changes (Fig. 4) shows that the response is predominantly local, yet
 with the "2012" experiment showing a more regional response. We here broadly define a local re-
 sponse as a situation where the grid points in close proximity to regions of sea ice change experience
 large changes in $\delta^{18}O_p$, and where grid points without sea ice change show no pronounced changes
 in $\delta^{18}O_p$. Similarly, a regional response is here used to describe a response where changes in $\delta^{18}O_p$
 175 both occur at grid points in close proximity to regions of sea ice changes and also at neighbouring
 grid points without sea ice changes.

Examination of the anomalies of isotopic composition of the water vapour yields insight into the
 isotopic composition of the Arctic moisture. Fig. 6 shows the anomaly of isotopic water vapour
 composition at the 850 hPa level (hereafter referred to as $\delta^{18}O_v$). The anomaly is plotted with

180 the 850-hPa level wind field anomaly overlaid. Similarly to the isotopic composition of precip-
itation, the isotopic composition of water vapour at the 850 hPa level reveals, for all experiments,
local anomalies at the same locations as anomalies of sea surface conditions occur. Locations with
decreased (increased) sea ice extent and concentration are co-located with locations of enriched (de-
pleted) water vapour. The wind vectors in Fig. 6 show that the changes in advection at the 850 hPa
185 level cannot explain the change in $\delta^{18}O_v$. Interestingly the highest wind anomalies are found in the
"2012" experiment which is also the experiment which displayed a more widespread and regional
isotopic response to sea ice changes. The slight increase in local wind anomalies could indicate that
advection is responsible for the larger spatial extent of the isotopic response.

Changes in local evaporation are here investigated based on the surface latent heat flux over ocean
190 and ice. To compare how changes in sea surface conditions change the amount of total local evapo-
ration, only locations with grid points of strongly reduced sea ice (change bigger than 20 %) were
selected and the amount of total latent heat flux per year for all grid points between $60^\circ N - 90^\circ N$
was calculated for all experiments. To account for different numbers of grid points with sea ice
change for each experiment the comparison to the CTRL run is done using identical locations of the
195 grid points, such that non-local effects in evaporation changes were excluded. As observed in Fig. 7
the amount of local evaporation is remarkably stronger for grid points where sea ice is reduced and
weaker where sea ice is increased. The number of gridpoints of reduced sea ice in each of the exper-
iments are as noted; 1980: 217, 1996: 444, 2007:1148, 2012: 2116. And the number of gridpoints of
increased sea ice; 1980: 1508, 1996: 1024, 2007:554, 2012: 437.

200 The two experiments with low sea ice extent ("2007" and "2012") have warmer temperatures,
more intense evaporation and higher values of $\delta^{18}O_v$ than the CTRL experiment. This contrasts the
two remaining experiments ("1980" and "1996") which have sea ice extent larger than the CTRL
run (based on 1979-2012 mean). In these experiments lower temperatures are observed as well as
less intense evaporation and lower values of $\delta^{18}O_v$ compared to the CTRL experiment. Our results
205 confirm that sea ice concentration and SST control the ability of the ocean to evaporate water to the
atmosphere.

4 Discussion

For isoCAM3, it is found that changes in sea ice and sea surface temperatures yield local changes
in the $\delta^{18}O$ of Arctic precipitation. The isotopic response is sensitive to the spatial configuration of
210 the sea surface conditions and the response of the changes are primarily local. Differences in the
isotopic response in Greenland and the rest of the Arctic thus exist for both vapour and precipitation.
The experiments show no changes of $\delta^{18}O$ for Greenland precipitation. Investigation of the vertical
distribution of $\delta^{18}O_v$ anomalies are shown in fig. 8 and 9. The zonal vertical cross sections of
temperature and $\delta^{18}O_v$ along the latitude $77^\circ N$ show that the changes in the $\delta^{18}O_v$ and temperature

Anomalies of annual mean $d18O_v$ advection

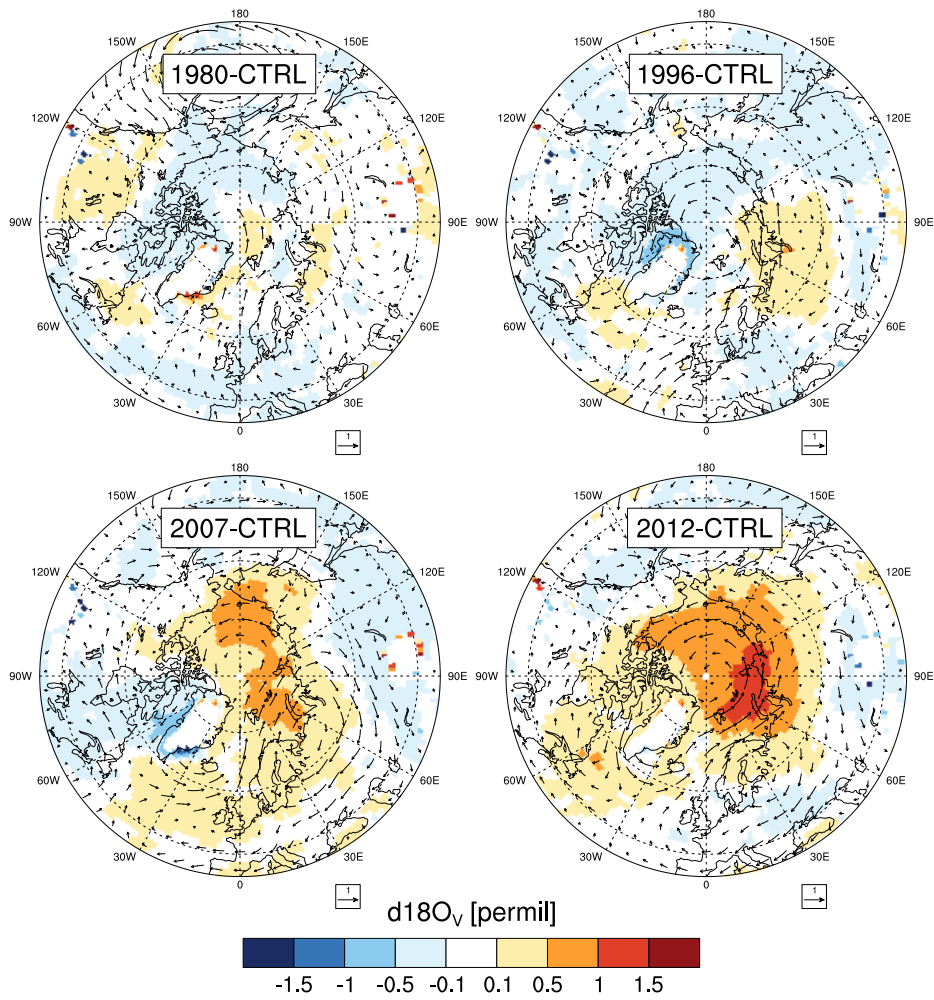


Figure 6. Annual mean anomalies of $\delta^{18}O_v$

Anomalies for the four simulations compared to the CTRL run. The arrows show the wind anomalies between the experiments and the CTRL run at the 850 hPa level.

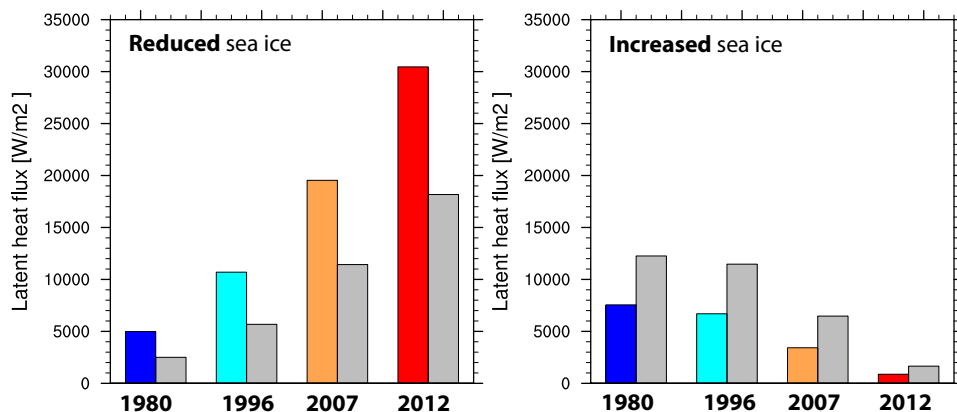


Figure 7. Latent heat flux for sea ice changes

Grid points of strongly reduced sea ice (anomaly bigger than 20 %) in each experiment were compared to identical grid points in the CTRL run and the amount of total latent heat flux per year for all grid points between $60^{\circ}N - 90^{\circ}N$ was calculated for both experiments and the CTRL run. The same was done for grid points of strongly increased sea ice. The coloured bars represent the latent heat flux over sea ice change regions for the different experiments and the grey bars adjacent to the coloured bar represent the latent heat flux for the identical grid points in the CTRL run.

215 are a surface based signals. This is also found in the spatial fields of $\delta^{18}O_v$ at different pressure levels
in the vertical (see appendix). The precipitation anomalies are not occurring together with anomalies
in the mid-troposphere $\delta^{18}O_v$ as seen in the vertical meridional cross sections of $\delta^{18}O_v$ (not shown).
While the anomalies of vapour and precipitation at the same location do not have to be linked, it still
suggest that the anomalies of precipitation are not connected to changes in air masses and large scale
220 transport but rather to local changes.

4.1 Are the moisture sources changing?

Based on the pronounced local structure of the isotopic response, and the evidence of an increase
in ocean evaporation when sea ice is reduced and SSTs are warmed (see Fig. 7), it is speculated

that the perturbations in the isotopic composition are caused by changes in the contribution from
225 local moisture sources. An increase in local Arctic Ocean evaporation would contribute with heavily
enriched water to the ambient vapour resulting in vapour that has a higher value of $\delta^{18}O_v$. This could
explain the simulated $\delta^{18}O_v$ anomalies. In the case of an increased sea ice cover, the decrease in the
contribution of local enriched water would result in ambient vapour with a lower value of $\delta^{18}O_v$.
This hypothesis is supported by observational studies of the impact of Arctic sea ice changes on the
230 isotopic composition of moisture (Klein et al., 2015; Kopec et al., 2016). Changes in evaporation of
local ocean water have also been suggested by modelling studies as important for sea ice induced
changes in $\delta^{18}O_p$ (Sime et al., 2013; Noone, 2004). Furthermore, an analysis of future warming
in the Arctic using state-of-the-art climate models showed changes in the hydrological cycle due
to Arctic warming and sea ice changes (Bintanja and Selten, 2014). In that study it was found that
235 moisture inflow from lower latitudes played a minor role, and the changes in the hydrological cycle
were mainly caused by strongly intensified local surface evaporation.

An alternative explanation for the simulated changes in $\delta^{18}O_v$ and $\delta^{18}O_p$ is that the changes occur
as result of changes in air mass characteristics. Reductions in the poleward temperature gradient
would reduce the cooling and condensation that air masses experience during the northward trans-
240 port. This would cause isotopic composition of the air masses to be less depleted. In this study, the
sea surface conditions effect on Arctic warming is clearly seen on the simulated surface air temper-
ature (T_{2m}) (see Fig. 3). Additionally also the vertical cross sections (fig. 8 and 9) cannot exclude
that the changes in the $\delta^{18}O_v$ is caused by changes in atmospheric temperature. Nevertheless, it is
difficult to explain the spatially very local effects of $\delta^{18}O_p$ as a cause of reduction in the poleward
245 temperature gradient. Yet, sea ice changes are connected to regions of cyclogenesis (Vihma, 2014;
Bader et al., 2011). Thus regions of open and warmer ocean surfaces might potentially steer cy-
clones to follow these paths and precipitate over the these regions, thereby creating a local signal of
 $\delta^{18}O_p$ changes. Our experimental design can not reveal the synoptical variability and the effects of
changed wind patterns are not clear from analysis of annual mean advection in the 850hPa layer in
250 6. The windspeed ($\sqrt{u^2 + v^2}$) at the 300 hPa level is weakened at midlatitudes in this study, which
indicates that the changes in sea surface conditions are influencing atmospheric circulation; yet no
clear connection to the changes in sea ice extent is found. Based on the considerations above it is
difficult to separate the effects of changes in temperature and changes in evaporation, and conse-
quently model simulations with moisture tracking features are suggested for further investigation of
255 this study. However, independent of the cause of the changes, it is found that changes in sea surface
conditions are important for the isotopic composition of non-Greenland $\delta^{18}O_p$ in the Arctic.

4.2 Influence on Greenland precipitation

Changes in the isotopic composition of Greenland precipitation are of special interest due to the ice
core research sites in this region. Interestingly, none of the sea ice perturbation experiments in this

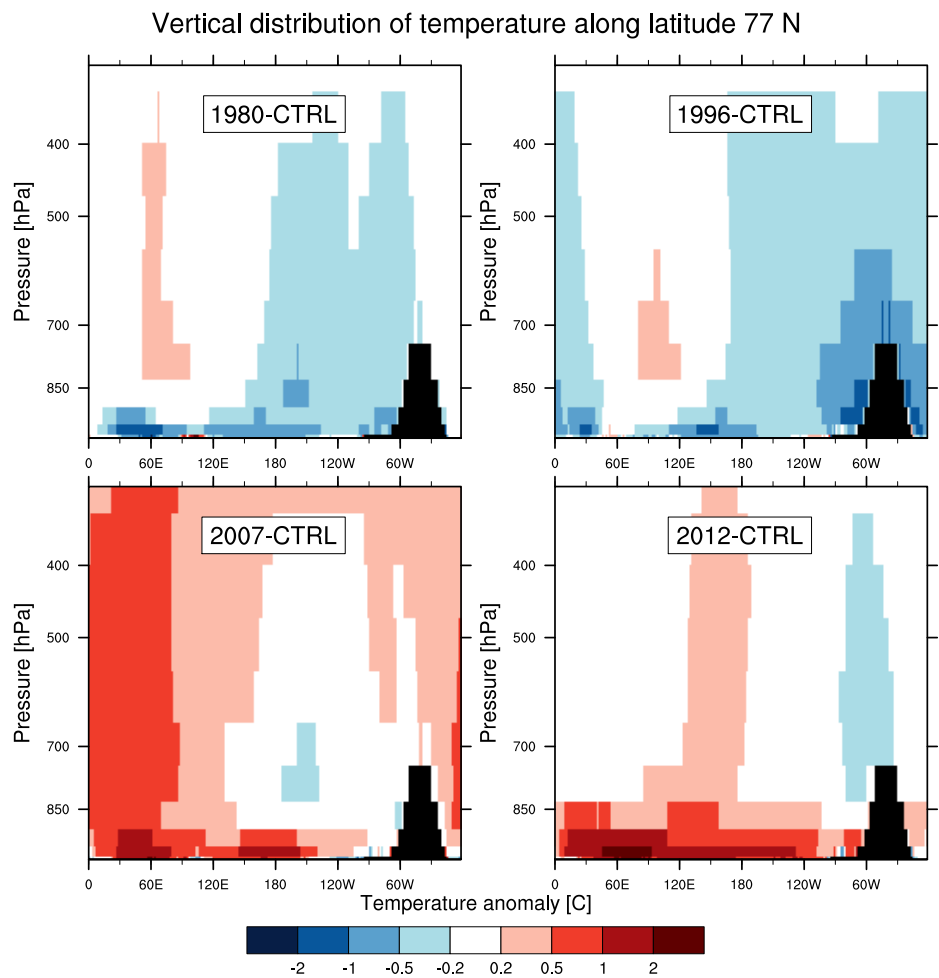


Figure 8. Vertical distribution of annual mean anomalies of temperature at the latitude band, $77^{\circ} N$. Annual mean anomalies for the four simulations compared to the CTRL run. Red and yellow colours represent an increase in temperature compared to the CTRL run. Blue colours represent a decrease in temperature compared to the CTRL run. The topography of Greenland is shown in black

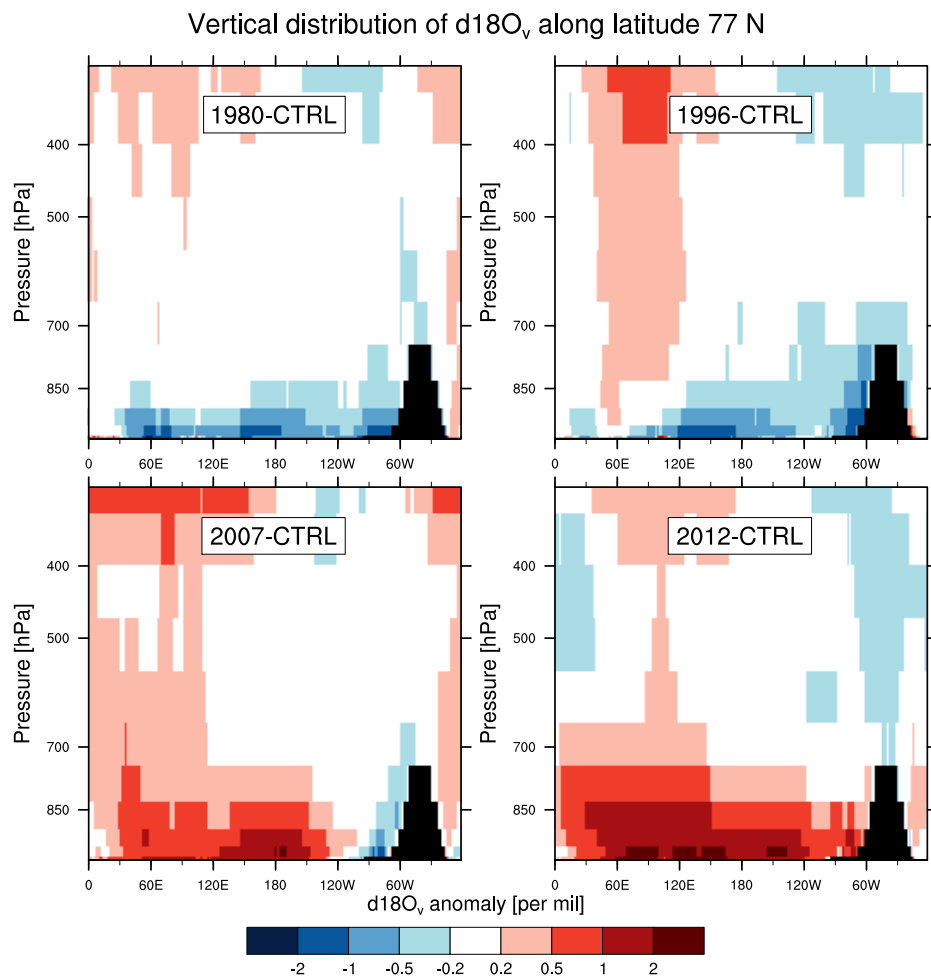


Figure 9. Vertical distribution of annual mean anomalies of $\delta^{18}O$ of vapour ($\delta^{18}O_v$) at the latitude band, 77° N

Annual mean anomalies for the four simulations compared to the CTRL run. Red and yellow colours represent an increase in $\delta^{18}O_p$ compared to the CTRL run. Blue colours represent a decrease in $\delta^{18}O_p$ compared to the CTRL run. The topography of Greenland is shown in black

260 study display $\delta^{18}O_p$ changes over Greenland. Thus the vertical distributions of T and $\delta^{18}O_v$ near the location of the ice core drilling site NEEM, Greenland ($\sim 77^\circ\text{N}$, 51°E) are used to investigate the differences in the response in Greenland and the rest of the Arctic. Fig. 8 and 9 show the circumpolar zonal vertical distribution of T and $\delta^{18}O_v$ at nearest gridpoint levels to NEEM. At non-Greenland locations the anomalies of T and $\delta^{18}O_v$ are surface based signals, sensitive to the local conditions. 265 However near NEEM, the Baffin Bay sea ice extent and associated simulated response in $\delta^{18}O_v$ are important for the $\delta^{18}O_v$ at NEEM. In experiment "2007" the Baffin Bay sea ice extent is increased compared to the mean values, while the near NEEM $\delta^{18}O_v$ displays negative anomalies of $\delta^{18}O_v$ in the range 0.2-1 ‰, this in spite of an overall Arctic enrichment. This suggests that the local conditions at Baffin Bay, and not the general Arctic conditions, are relevant for studying the $\delta^{18}O_v$ 270 response to sea ice changes at NEEM. Modern observations of the isotopic composition of snow and water vapour from NEEM also show that variations in modern values of $\delta^{18}O$ correlate with conditions in Baffin Bay sea ice extent Steen-Larsen et al. (2011).

The lack of sensitivity of the Greenland $\delta^{18}O_p$ to changes in Arctic Ocean surface conditions is argued to be related to the topography of Greenland. Specifically, the steep slopes of the ice sheet 275 margin are associated with substantial orographic enhancement of precipitation and depletion of air mass water vapour content. Processes controlling the Greenland $\delta^{18}O_p$ might be decoupled from the processes influencing the $\delta^{18}O_p$ over the Arctic ocean. The Greenland katabatic wind blocking effect (Noel et al., 2014) might also play a role in blocking of low level moisture to Greenland.

We note that our experiment does not exhibit the strong warming observed over Greenland in 280 2012. The observed 2012 Greenland melting was attributed to the following key factors; the North American heat wave, transitions in the Arctic Oscillation and transport of warm air and vapour via an atmospheric river (Neff et al., 2014; Bonne et al., 2014). Forcing the model with only oceanic conditions can thus not create a similar atmospheric-induced warming.

In contrast to the results of this study, Sime et al. (2013) simulated 2 – 3‰ changes in central 285 Greenland $\delta^{18}O_p$ for extremely warm climates with SST and sea ice conditions created from coupled model experiment forced by large increases in CO_2 . The main differences between the simulations in this study and in the study by Sime et al. (2013) are related to the distribution and magnitude of sea ice and SST changes especially near northern Greenland.

In the study by Sime et al. (2013) sea ice and SST changes also occur in the region north of 290 Greenland. Also the magnitude of Arctic SST anomalies are $8-10^\circ\text{C}$ whereas the simulations in this study have anomalies of $3-5^\circ\text{C}$. These differences are compelling as our experiment "2012" with the largest prescribed SST anomalies and sea ice changes also is the only experiment that simulates a regional isotopic response. This indicates that the magnitude of SST changes might control not only the amount of local evaporation, but also the regional extent of the isotopic response. Hence, it 295 is possible that the simulated changes of $\delta^{18}O_p$ by (Sime et al., 2013) have a regional extent due to the same reasons as experiment "2012".

Warming of the lower troposphere and associated weakening of the inversion layer might be important in controlling the extent of the isotopic response. As sea ice removal is connected to intense warming of the lower troposphere (Screen et al., 2012; Deser et al., 2010), it could be speculated that this warming is controlling the extent of the isotopic response. This would be possible as a weaker inversion layer allows atmospheric convection, and Abbot and Tziperman (2008) have shown that this can occur at high-latitudes in sea ice free regions in winter. Further investigation of the mechanism causing this change requires further idealized experiments following a similar design to Noone (2004), so that a systematic investigation of the atmospheric processes influencing the isotopic composition of moisture is possible.

5 Conclusions

The aim of this study was to investigate whether changes in sea ice and sea surface temperatures derived from observed anomalies can influence the isotopic composition of precipitation in the Arctic. Results are presented from isoCAM3 an isotope-equipped AGCM, forced with different distributions of Arctic sea ice changes and associated SST from the ERA-interim re-analysis product. These simulations show that changes in sea ice and sea surface conditions influence the isotopic composition of Arctic precipitation with regional changes of $\delta^{18}O_p$ of up to 3‰ in the Barents Sea region. However, no changes are found for Greenland; a region relevant for isotope records from ice cores. For all experiments it is found that regions of increased (decreased) sea ice extent and concentration results in enriched (depleted) $\delta^{18}O$ values of precipitation.

The $\delta^{18}O$ response to the ocean conditions is primarily local. Changes in sea ice and sea surface temperatures yield local surface based anomalies of $\delta^{18}O$ of vapour. Differences in the isotopic response in Greenland and the rest of the Arctic thus exist for both vapour and precipitation. Within the same experiment large changes in $\delta^{18}O$ are observed over some regions and no changes over other regions. The geographical variations in the $\delta^{18}O$ response to changes in Arctic sea surface conditions show that the isotopic composition of Arctic precipitation is sensitive to the spatial distribution of the sea ice and SST changes, however not at Greenland. This means that different distributions of similar sea ice areas can produce very different $\delta^{18}O_p$ values at the same location. Or conversely, that different locations respond very differently in $\delta^{18}O_p$ to the same total Arctic sea ice extent. The isotopic composition of Greenland precipitation is unaffected by the imposed changes in central Arctic sea ice cover in all experiments. Only conditions near Baffin Bay influence Greenland. As many ice cores originate from the Greenland Ice Sheet this is an important result for the interpretation of isotope records.

Previous studies have shown that large changes in the state of sea ice and SST conditions influences the isotope composition over Greenland (Sime et al., 2013) and Antarctica (Noone, 2004) but this study is the first model experiment to show that minor (relative to Sime et al. (2013)) perturba-

tions in the sea ice cover and SST under present-day climate conditions can yield significant changes in the isotopic composition of precipitation in the Arctic, while at the same time not changing conditions in Greenland.

335 *Acknowledgements.* We thank the two anonymous reviewers for helpful comments and suggestions. The research leading to these results has received funding from the European Research Council under the European Union’s Seventh Framework Programme (FP7/2007-2013) / ERC grant agreement number 610055 as part of the ice2ice project. The authors acknowledge the support of the Danish National Research Foundation through the Centre for Ice and Climate, Niels Bohr Institute.

340 6 Appendix

Annual mean $\delta^{18}O_p$ for the CTRL run is compared to observations of present day annual mean $\delta^{18}O$ from Greenland ice cores (Vinther et al., 2010). Fig. 10 show that the isoCAM3 model has an annual mean positive bias of $\delta^{18}O$.

Annual mean $\delta^{18}O_p$ compared to observations

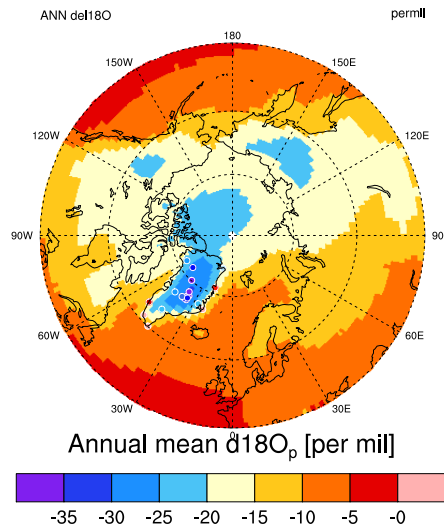


Figure 10. Annual mean $\delta^{18}O_p$ for the CTRL run compared to observations

Annual mean $\delta^{18}O_p$ for the CTRL run compared to observations. The circles represent annual mean values from ice core and GNIP observations.

No change in annual mean precipitation is found for each of the experiments compared to the
 345 CTRL run as shown in Fig. 11.

Anomalies of annual mean precipitation

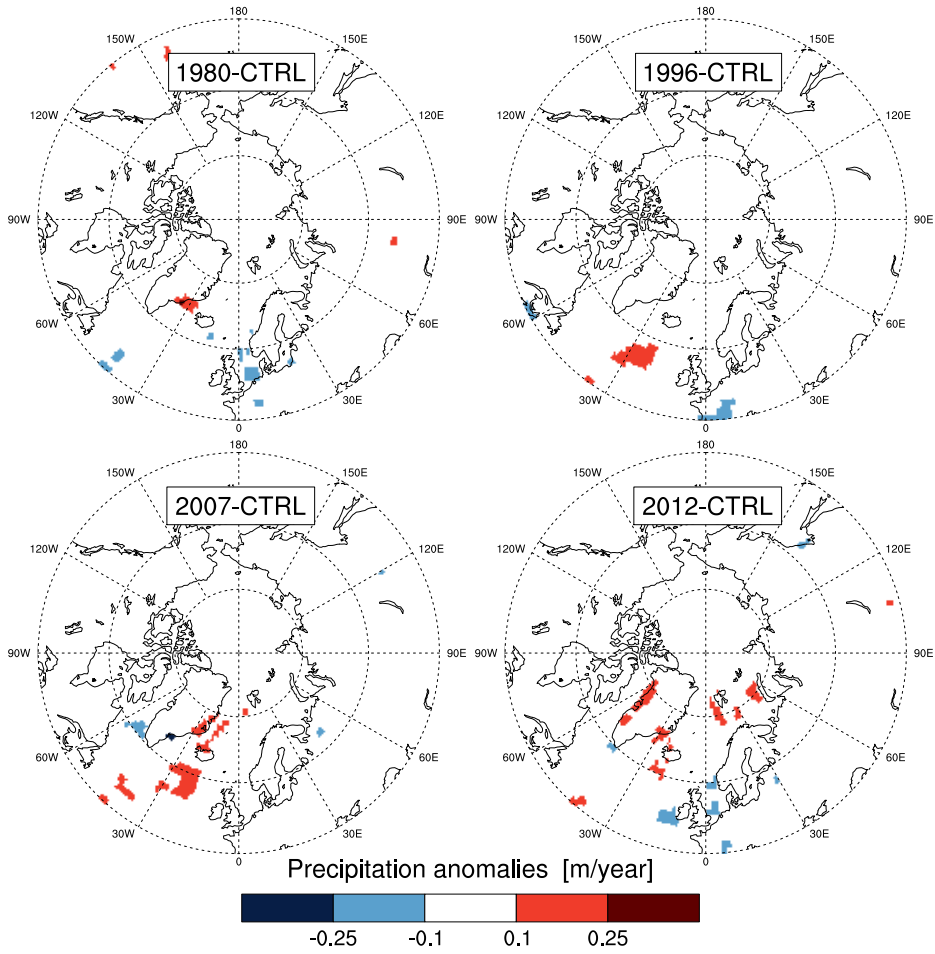


Figure 11. Annual mean anomalies of precipitation

Anomalies for the four simulations compared to the CTRL run.

The spatial distributions of the anomalies of $\delta^{18}O_v$ at the 950 hPa level and 700 hPa level (Fig. 12 and 13) show that the anomalies of $\delta^{18}O_v$ are mostly found at surface levels for the entire Arctic region.

At 950 hPa level: Anomalies of annual mean $d18O_v$

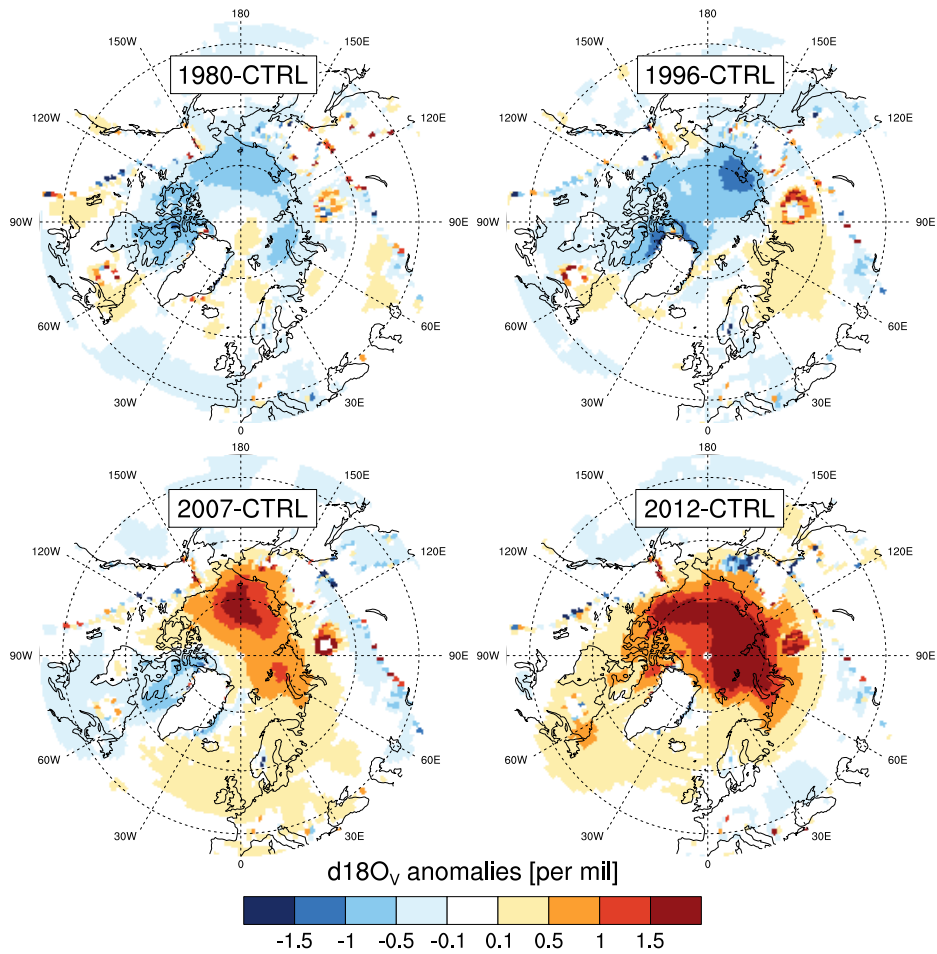


Figure 12. Annual mean anomalies of $\delta^{18}O_v$

Anomalies for the four simulations compared to the CTRL run. The arrows show the wind anomalies between the experiments and the CTRL run at the 950 hPa level.

At 700 hPa level: Anomalies of annual mean $d18O_v$

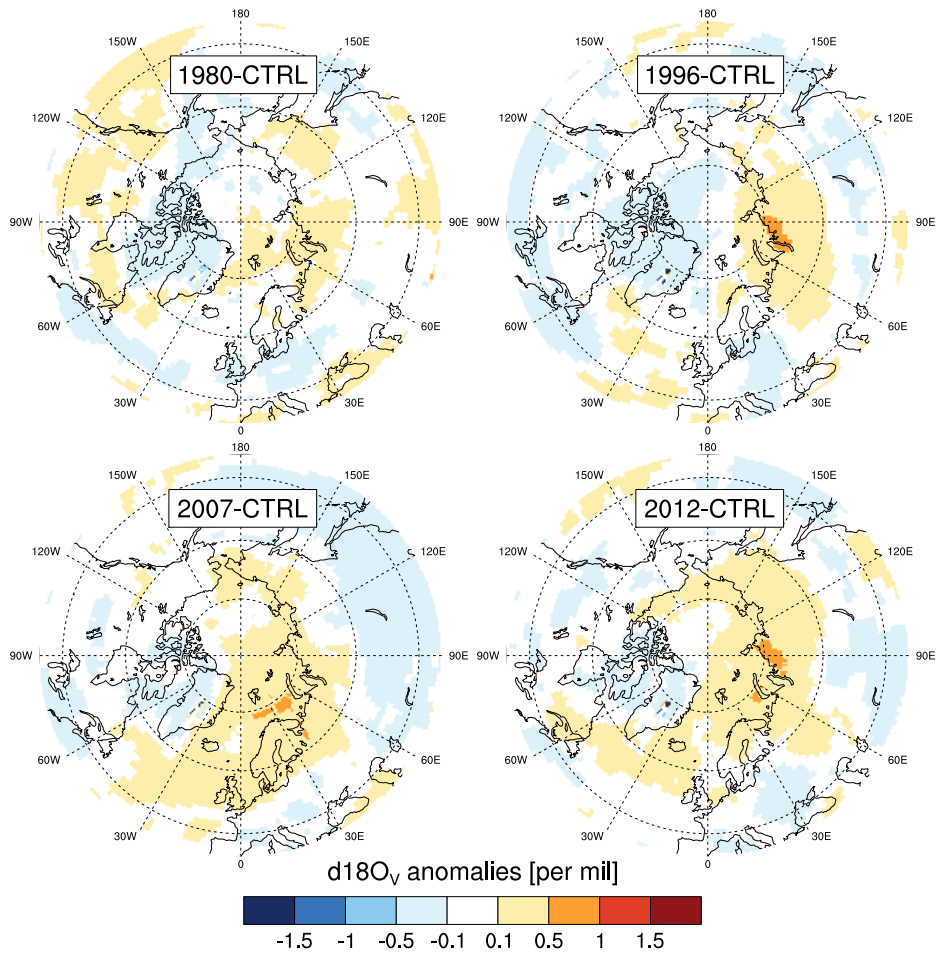


Figure 13. Annual mean anomalies of $\delta^{18}O_v$

Anomalies for the four simulations compared to the CTRL run. The arrows show the wind anomalies between the experiments and the CTRL run at the 700 hPa level.

References

- 350 Abbot, D. S. and Tziperman, E.: Sea ice, high-latitude convection, and equable climates, *Geophysical Research Letters*, 35, 2008.
- Bader, J., Mesquita, M. D. S., Hodges, K. I., Keenlyside, N., Osterhus, S., and Miles, M.: A review on Northern Hemisphere sea-ice, storminess and the North Atlantic Oscillation: observations and projected changes, *Atmospheric Research*, 101, 809–834, 2011.
- 355 Bintanja, R. and Selten, F.: Future increases in Arctic precipitation linked to local evaporation and sea-ice retreat, *Nature*, 509, 479–482, 2014.
- Blüthgen, J., Gerdes, R., and Werner, M.: Atmospheric response to the extreme Arctic sea ice conditions in 2007, *Geophysical Research Letters*, 39, doi:10.1029/2011GL050486, <http://doi.wiley.com/10.1029/2011GL050486>, 2012.
- 360 Bonne, J.-L. L., Masson-Delmotte, V., Cattani, O., Delmotte, M., Risi, C., Sodemann, H., and Steen-Larsen, H. C.: The isotopic composition of water vapour and precipitation in Ivittuut, southern Greenland, *Atmospheric Chemistry and Physics*, 14, 4419–4439, doi:10.5194/acp-14-4419-2014, <http://www.atmos-chem-phys.net/14/4419/2014/>, 2014.
- Budikova, D.: Role of Arctic sea ice in global atmospheric circulation: A review, *Global and Planetary Change*, 68, 149–163, doi:10.1016/j.gloplacha.2009.04.001, <http://linkinghub.elsevier.com/retrieve/pii/S0921818109000654>, 2009.
- 365 Collins, W. D., Rasch, P. J., Boville, B. A., Hack, J. J., McCaa, J. R., Williamson, D. L., Briegleb, B. P., Bitz, C. M., Lin, S.-J. J., and Zhang, M. H.: The formulation and atmospheric simulation of the Community Atmosphere Model version 3 (CAM3), *JOURNAL OF CLIMATE*, 19, 2144–2161, doi:10.1175/JCLI3760.1,
- 370 2006.
- Dansgaard, W.: Stable Isotopes in Precipitation, *Tellus*, 16, 436–468, doi:10.1111/j.2153-3490.1964.tb00181.x, <http://doi.wiley.com/10.1111/j.2153-3490.1964.tb00181.x>, 1964.
- Dee, D. P., Uppala, S. M., Simmons, A. J., Berrisford, P., Poli, P., Kobayashi, S., Andrae, U., Balmaseda, M. A., Balsamo, G., Bauer, P., Bechtold, P., Beljaars, A. C. M., van de Berg, L., Bidlot, J., Bormann, N., Delsol, C.,
- 375 Dragani, R., Fuentes, M., Geer, A. J., Haimberger, L., Healy, S. B., Hersbach, H., Holm, E. V., Isaksen, L., Kallberg, P., Koehler, M., Matricardi, M., McNally, A. P., Monge-Sanz, B. M., Morcrette, J. J., Park, B. K., Peubey, C., de Rosnay, P., Tavolato, C., Thepaut, J. N., and Vitart, F.: The ERA-Interim reanalysis: configuration and performance of the data assimilation system, *Quarterly Journal of The Royal Meteorological Society*, 137, 553–597, 2011.
- 380 Deser, C., Tomas, R., Alexander, M., and Lawrence, D.: The seasonal atmospheric response to projected Arctic sea ice loss in the late twenty-first century, *Journal of Climate*, 23, 333–351, 2010.
- Divine, D., Isaksson, E., Martma, T., a.J. Meijer, H., Moore, J., Pohjola, V., van de Wal, R. S., and Godtliessen, F.: Thousand years of winter surface air temperature variations in Svalbard and northern Norway reconstructed from ice-core data, *Polar Research*, 30, 1–12, doi:10.3402/polar.v30i0.7379, <http://www.polarresearch.net/index.php/polar/article/view/7379>, 2011.
- 385 Fauria, M. M., Grinsted, A., Helama, S., Moore, J., Timonen, M., Martma, T., Isaksson, E., and Eronen, M.: Unprecedented low twentieth century winter sea ice extent in the Western Nordic Seas since AD 1200, *Climate Dynamics*, 34, 781–795, 2010.

- Fetterer, F., Knowles, K., Meier, W., and Savoie, M.: Sea ice index, Natl Snow and Ice Data Center, Boulder, CO) Available at <http://nsidc.org/data/g02135.htm>. Accessed February, 9, 2009, 2002.
- 390 Johnsen, S. J., Dansgaard, W., and White, J. W. C.: The origin of Arctic precipitation under present and glacial conditions, *Tellus B*, 41B, 452–468, doi:10.1111/j.1600-0889.1989.tb00321.x, <http://doi.wiley.com/10.1111/j.1600-0889.1989.tb00321.x>, 1989.
- Klein, E. S., Cherry, J., Young, J., Noone, D., Leffler, A., and Welker, J.: Arctic cyclone water vapor isotopes support past sea ice retreat recorded in Greenland ice, *Scientific reports*, 5, 2015.
- 395 Kopec, B. G., Feng, X., Michel, F. A., and Posmentier, E. S.: Influence of sea ice on Arctic precipitation, *Proceedings of the National Academy of Sciences*, 113, 46–51, 2016.
- Ku, M., Monaghan, A. J., Battisti, D. S., Küttel, M., Steig, E. J., Ding, Q., Monaghan, A. J., Battisti, D. S., Ku, M., Monaghan, A. J., and Battisti, D. S.: Seasonal climate information preserved in West Antarctic ice core water isotopes: Relationships to temperature, large-scale circulation, and sea ice, *Climate dynamics*, 39, 400 1841–1857, doi:10.1007/s00382-012-1460-7, 2012.
- Li, C., Battisti, D. S., and Bitz, C. M.: Can North Atlantic Sea Ice Anomalies Account for Dansgaard-Oeschger Climate Signals?*, *Journal of Climate*, 23, 5457–5475, 2010.
- Liu, Z., Carlson, A. E., He, F., Brady, E. C., Otto-Bliesner, B. L., Briegleb, B. P., Wehrenberg, M., Clark, 405 P. U., Wu, S., Cheng, J., and Others: Younger Dryas cooling and the Greenland climate response to CO₂, *Proceedings of the National Academy of Sciences*, 109, 11 101–11 104, 2012.
- Liu, Z., Wen, X., Brady, E. C., Otto-Bliesner, B., Yu, G., Lu, H., Cheng, H., Wang, Y., Zheng, W., Ding, Y., Others, Edwards, R. L., Cheng, J., Liu, W., and Yang, H.: Chinese cave records and the East Asia summer monsoon, *Quaternary Science Reviews*, 83, 115–128, doi:10.1016/j.quascirev.2013.10.021, 2014.
- 410 Magnusdottir, G., Deser, C., and Saravanan, R.: The effects of North Atlantic SST and sea ice anomalies on the winter circulation in CCM3. Part I: Main features and storm track characteristics of the response, *Journal of Climate*, 17, 857–876, 2004.
- Neff, W., Compo, G. P., Martin Ralph, F., and Shupe, M. D.: Continental heat anomalies and the extreme melting of the Greenland ice surface in 2012 and 1889, *Journal of Geophysical Research: Atmospheres*, 119, 415 6520–6536, 2014.
- Noel, B., Fettweis, X., Van De Berg, W., Van Den Broeke, M., and Ericum, M.: Sensitivity of Greenland Ice Sheet surface mass balance to perturbations in sea surface temperature and sea ice cover: a study with the regional climate model MAR, *Cryosphere (The)*, 8, 1871–1883, 2014.
- Noone, D.: Sea ice control of water isotope transport to Antarctica and implications for ice core interpretation, 420 *Journal of Geophysical Research*, 109, D07 105, doi:10.1029/2003JD004228, <http://doi.wiley.com/10.1029/2003JD004228>, 2004.
- Noone, D. and Sturm, C.: Comprehensive Dynamical Models of Global and Regional Water Isotope Distributions, *Isoscapes: Understanding movement, pattern, and process on Earth through isotope mapping*, p. 195, 2010.
- 425 Opel, T., Fritzsche, D., and Meyer, H.: Eurasian Arctic climate over the past millennium as recorded in the Akademii Nauk ice core (Severnaya Zemlya), *Climate of the Past*, 9, 2379–2389, 2013.

- Pausata, F. S. R., Battisti, D. S., Nisancioglu, K. H., and Bitz, C. M.: Chinese stalagmite $\delta^{18}\text{O}$ controlled by changes in the Indian monsoon during a simulated Heinrich event, *Nature Geoscience*, 4, 474–480, doi:10.1038/ngeo1169, <http://www.nature.com/doi/finder/10.1038/ngeo1169>, 2011.
- 430 Screen, J. a., Deser, C., and Simmonds, I.: Local and remote controls on observed Arctic warming, *Geophysical Research Letters*, 39, n/a–n/a, doi:10.1029/2012GL051598, <http://doi.wiley.com/10.1029/2012GL051598>, 2012.
- Screen, J. a., Deser, C., Simmonds, I., and Tomas, R.: Atmospheric impacts of Arctic sea-ice loss, 1979–2009: separating forced change from atmospheric internal variability, *Climate Dynamics*, doi:10.1007/s00382-013-1830-9, <http://link.springer.com/10.1007/s00382-013-1830-9>, 2013a.
- 435 Screen, J. a., Simmonds, I., Deser, C., and Tomas, R.: The Atmospheric Response to Three Decades of Observed Arctic Sea Ice Loss, *Journal of Climate*, 26, 1230–1248, doi:10.1175/JCLI-D-12-00063.1, <http://journals.ametsoc.org/doi/abs/10.1175/JCLI-D-12-00063.1>, 2013b.
- Sewall, J. O. and Fricke, H. C.: Andean-scale highlands in the Late Cretaceous Cordillera of the North American western margin, *Earth and Planetary Science Letters*, 362, 88–98, 2013.
- 440 Sime, L. C., Risi, C., Tindall, J. C., Sjolte, J., Wolff, E. W., Masson-Delmotte, V., and Capron, E.: Warm climate isotopic simulations: what do we learn about interglacial signals in Greenland ice cores?, *Quaternary Science Reviews*, 67, 59–80, doi:10.1016/j.quascirev.2013.01.009, <http://linkinghub.elsevier.com/retrieve/pii/S0277379113000188>, 2013.
- 445 Sjolte, J., Hoffmann, G., Johnsen, S. J., Vinther, B. M., Masson-Delmotte, V., and Sturm, C.: Modeling the water isotopes in Greenland precipitation 1959–2001 with the meso-scale model REMO-iso, *Journal of Geophysical Research*, 116, D18 105, doi:10.1029/2010JD015287, <http://doi.wiley.com/10.1029/2010JD015287>, 2011.
- Sodemann, H., Masson-Delmotte, V., Schwierz, C., Vinther, B. M., and Wernli, H.: Interannual variability of Greenland winter precipitation sources: 2. Effects of North Atlantic Oscillation variability on stable isotopes in precipitation, *Journal of Geophysical Research-Atmospheres*, 113, 1–21, doi:10.1029/2007JD009416, <http://www.agu.org/pubs/crossref/2008/2007JD009416.shtml>, 2008a.
- 450 Sodemann, H., Schwierz, C., and Wernli, H.: Interannual variability of Greenland winter precipitation sources: Lagrangian moisture diagnostic and North Atlantic Oscillation influence, *Journal of Geophysical Research - Atmospheres*, 113, doi:10.1029/2007JD008503, 2008b.
- 455 Speelman, E. N., Sewall, J. O., Noone, D., Huber, M., der Heydt, A. V., Damsté, J. S., Reichart, G.-J., von der Heydt, A., Damsté, J. S., and Reichart, G.-J.: Modeling the influence of a reduced equator-to-pole sea surface temperature gradient on the distribution of water isotopes in the Early/Middle Eocene, *Earth and Planetary Science Letters*, 298, 57–65, doi:10.1016/j.epsl.2010.07.026, <http://linkinghub.elsevier.com/retrieve/pii/S0012821X10004644>, 2010.
- 460 Steen-Larsen, H. C., Masson-Delmotte, V., Sjolte, J., Johnsen, S. J., Vinther, B. M., Bréon, F.-M., Clausen, H., Dahl-Jensen, D., Falourd, S., Fettweis, X., et al.: Understanding the climatic signal in the water stable isotope records from the NEEM shallow firn/ice cores in northwest Greenland, *Journal of Geophysical Research: Atmospheres*, 116, 2011.
- 465 Sturm, C., Zhang, Q., and Noone, D.: An introduction to stable water isotopes in climate models: benefits of forward proxy modelling for paleoclimatology, *Climate of the past*, 6, 115–129, 2010.

- Tharammal, T., Paul, a., Merkel, U., and Noone, D.: Influence of Last Glacial Maximum boundary conditions on the global water isotope distribution in an atmospheric general circulation model, *Climate of the Past*, 9, 789–809, doi:10.5194/cp-9-789-2013, <http://www.clim-past.net/9/789/2013/>, 2013.
- 470 Vihma, T.: Effects of Arctic sea ice decline on weather and climate: A review, *Surveys in Geophysics*, 35, 1175–1214, 2014.
- Vinther, B. M., Jones, P. D., Briffa, K. R., Clausen, H. B., Andersen, K. K., Dahl-Jensen, D., and Johnsen, S. J.: Climatic signals in multiple highly resolved stable isotope records from Greenland, *Quaternary Science Reviews*, 29, 522–538, doi:10.1016/j.quascirev.2009.11.002, <http://linkinghub.elsevier.com/retrieve/pii/S0277379109003655>, 2010.
- 475 White, J. W. C., Barlow, L. K., Fisher, D., Grootes, P., Jouzel, J., Johnsen, S. J., Stuiver, M., and Clausen, H.: The climate signal in the stable isotopes of snow from Summit, Greenland: Results of comparisons with modern climate observations, *Journal of Geophysical Research-Oceans*, 102, 26 425–26 439, 1997.